HHS Public Access

Author manuscript

J Thorac Oncol. Author manuscript; available in PMC 2023 March 01.

Published in final edited form as:

J Thorac Oncol. 2023 March ; 18(3): 350–368. doi:10.1016/j.jtho.2022.11.008.

An Interleukin-15 Superagonist Enables Antitumor Efficacy of Natural Killer Cells Against All Molecular Variants of SCLC

Kristen Fousek, PhD[a], **Lucas A. Horn, PhD**[a], **Haiyan Qin, MS**[a], **Madeline Dahut, BS**[a], **Masafumi Iida, MD, PhD**[a], **Dan Yacubovich, BS**[a], **Duane H. Hamilton, PhD**[a], **Anish Thomas, MD**[b], **Jeffrey Schlom, PhD**[a], **Claudia Palena, PhD**[a,*]

[a]Center for Immuno-Oncology, Center for Cancer Research, National Cancer Institute, National Institutes of Health, Bethesda, Maryland

[b]Developmental Therapeutics Branch, Center for Cancer Research, National Cancer Institute, National Institutes of Health, Bethesda, Maryland

Abstract

Introduction: SCLC is a highly aggressive tumor with a 5-year survival rate of less than 6%. A heterogeneous disease, SCLC is classified into four subtypes that include tumors with neuroendocrine and non-neuroendocrine features. Immune checkpoint blockade therapy has been recently added for the frontline treatment of SCLC; immune checkpoint blockade, however, has only led to modest clinical improvements. The lack of clinical benefit in a cancer type known to have a high tumor mutational burden has been attributed to poor T-cell infiltration and low expression of MHC-class I in most SCLC tumors. In an attempt to devise a more effective immunotherapeutic regimen, this study investigated an alternate approach on the basis of the use of the clinical-stage interleukin-15 superagonist, N-803.

Methods: Preclinical models of SCLC spanning all molecular subtypes were used to evaluate the susceptibility of SCLC to natural killer (NK)-mediated lysis in vitro, including NK cells activated by N-803. Antitumor activity of N-803 was evaluated in vivo with a xenograft model of SCLC.

*Corresponding author. Address for correspondence: Claudia Palena, PhD, Center for Immuno-Oncology, Center for Cancer Research, National Cancer Institute, National Institutes of Health, Bethesda, MD 20892. palenac@mail.nih.gov.

CRediT Authorship Contribution Statement

Kristen Fousek: Conceptualization, Data curation, Investigation, Methodology, Formal analysis, Writing—original draft, Writing—review and editing.

Lucas A. Horn: Data curation, Investigation, Methodology, Formal analysis.

Haiyan Qin: Investigation, Methodology.

Madeline Dahut: Investigation, Formal analysis. **Masafumi Iida:** Investigation, Formal analysis.

Dan Yacubovich: Investigation, Formal analysis. **Duane H. Hamilton:** Investigation, Methodology, Formal analysis.

Anish Thomas: Resources, Data curation.

Jeffrey Schlom: Supervision, Writing—review and editing.

Claudia Palena: Conceptualization, Supervision, Data curation, Formal analysis, Writing—original draft, Writing—review and editing.

Supplementary Data

Note: To access the supplementary material accompanying this article, visit the online version of the *Journal of Thoracic Oncology* at www.jto.org and at https://doi.org/10.1016/j.jtho.2022.11.008.

Disclosure: The National Cancer Institute, National Institutes of Health has an ongoing CRADA with ImmunityBio, Inc. Dr. Palena discloses spouse's employment and holdings in MacroGenics, Inc. The remaining authors declare no conflict of interest.

Results: In vitro and in vivo data revealed differences in susceptibility of SCLC subtypes to lysis by NK cells and that NK cells activated by N-803 effectively lyse SCLC tumor cells across all variant subtypes, regardless of their expression of MHC-class I.

Conclusions: These findings highlight the potential of a novel immune-based intervention using a cytokine-based therapeutic option for the treatment of SCLC. We hypothesize that N-803 may provide benefit to most patients with SCLC, including those with immunologically cold tumors lacking MHC expression.

Keywords

Small cell lung cancer; Immunotherapy; NK-cell therapy; N-803

Introduction

SCLC, which accounts for approximately 15% of all lung cancers, is an aggressive cancer type with a 5-year overall survival rate of only 6%.[1] Patients generally respond well to initial regimens of platinum-etoposide–based chemotherapy, but most experience relapse within the first year. Historically, SCLC has been considered a primarily neuroendocrine (NE) tumor, with a subset of tumors designated as non-NE (non-NE), which lack classical NE markers such as chromogranin, synaptophysin, and NCAM1. More recently, these two broad categories have been further defined at the molecular level, in which four subtypes of SCLC have been described on the basis of the expression of four major transcriptional regulators. Tumors expressing the transcription factors ASCL1 or NEUROD1 constitute the NE subset, which makes up approximately 80% of the tumors; the remaining minority of non-NE SCLC tumors are those which express either the POU2F3 or the YAP1 transcription factors.[2] The molecular classification of SCLC revealed high levels of intratumoral heterogeneity in SCLC[3,4] and that subpopulations of non-NE, $YAP1^{POS}$ tumor cells, which are more resistant to therapeutic intervention,[5] are selected by chemotherapy treatment.[6]

Immune checkpoint blockade (ICB) with monoclonal antibodies targeting programmed cell death protein 1 (PD-1), or its ligand, programmed death-ligand 1 (PD-L1), has been recently added as frontline therapy in the treatment of SCLC; however, despite the high tumor mutation burden, ICB has only made modest improvements in overall survival.[7,8] In a retrospective analysis of the IMpower133 trial comparing the addition of atezolizumab, a PD-L1 antibody, to frontline standard of care chemotherapy, a trend was observed that the greatest benefit was provided to the specific subset of SCLC lacking expression of ASCL1, NEUROD1, and POU2F3. These tumors were described as SCLC-inflamed as they exhibited the highest expression of T cell and interferon-γ (IFN-γ) response genes, most likely contributing to the improved ICB efficacy observed in these patients.[6] The study suggested that the potential benefit of ICB immunotherapy may only be achieved in a few patients with SCLC who have a relatively activated and immune “hot” tumor microenvironment.[6,9,10]

Unlike T cells, natural killer (NK) cells have been less evaluated in SCLC. The functionality of the NK cells relies on the balance of activating and inhibitory signals received through the NK receptors, including the activating natural cytotoxicity receptors NKp30, NKp44,

or NKp46, and NKG2 family members, most notably NKG2D, and inhibitory receptors of the KLRG family that provide repressive signals by binding to MHC-class I molecules or cadherins.[11,12] With this knowledge, it was hypothesized that although a few (approximately 17%) tumors that express high levels of MHC-class I would be resistant to NK therapy, the NK cells may provide efficacy as an immunotherapy for the remaining 83% of SCLC tumors of the other subtypes, which express low levels of MHC-class I and are immunologically "cold," making them less likely to respond to ICB therapy.

This study investigated the utility of an alternative immunotherapy approach using an NK-based therapy for the treatment of SCLC of all subtypes using several human SCLC tumor cell line models. On observation that only a subset of tumors were sensitive to NK-mediated lysis, the addition of interleukin-15 (IL-15) cytokine, which is known to cause activation and proliferation of both NK and $CD8^{POS}$ T cells and to impart improvements in the cytotoxic capacity of these cells, was investigated.[13] IL-15 was delivered by N-803 (previously ALT-803), a clinical-stage superagonist complex of a mutant human IL-15 (IL15N72D) combined with the sushi domain of hIL15Rα and fused to an IgG1 Fc domain.[14–16] In vitro and in vivo data indicated that IL-15 superagonist–activated NK cells effectively lyse SCLC tumor cells across all variant subtypes, including those previously completely refractory to traditional NK cell lysis. These results highlight the potential of N-803 as an alternative immune-based intervention for the treatment of SCLC.

Materials and Methods

Cell Lines and Reagents

Human cell lines DMS79, NCI-H69, NCI-H1048, NCI-H526, and NCI-H841 were obtained from the American Type Culture Collection (Manassas, VA). Human cell lines NCI-H524, NCI-H82, and DMS114 were kindly provided by Dr. Anish Thomas, National Cancer Institute (NCI). All cells were cultured as recommended by the American Type Culture Collection. N-803 was provided by ImmunityBio Inc., under a Cooperative Research and Development Agreement (CRADA) with the NCI/National Institutes of Health (NIH). Recombinant human IL-15 and IL-2 were purchased from PeproTech (Cranbury, NJ).

Peripheral Blood From Healthy Donors and Patients With SCLC

Deidentified peripheral blood mononuclear cell (PBMC) samples were obtained from healthy volunteers who provided written informed consent at the NIH Clinical Center Blood Bank (ClinicalTrials.gov #NCT00001846). Viably frozen PBMCs were obtained from three patients with SCLC enrolled in NCI protocol #14-C-0105; ClinicalTrials.gov #NCT02146170. NIH Institutional Review Board, Office of Human Subjects Research Protections at the NCI approved the studies; all patients provided written informed consent. Patient PBMCs were cultured in Roswell Park Memorial Institute 1640 Medium with 10% human AB serum added.

Immunofluorescent Staining

A SCLC tumor microarray (LC818c) was purchased from US Biomax (Derwood, MD). Antigen retrieval was performed by microwaving 45 seconds at 100% power followed

by 15 minutes at 20% power in pH6 buffer (Akoya Biosciences, Marlborough, MA). After blocking in BLOXALL solution (Vector Laboratories, Burlingame, CA), primary antibodies against human NCAM1 (clone MRQ-42, 1:250, Millipore Sigma, Burlington, MA), MHC-class I (clone EMR8–5, 1:1000, Abcam, Waltham, MA), ASCL1 (clone D-7, 1:1000, Santa Cruz Biotechnology, Dallas, TX), NEUROD1 (clone EPR17084, 1:400, Abcam), POU2F3 (polyclonal, 1:200, Novus Biologicals, Centennial, CO), YAP1 (clone 63.7, 1:1000, Santa Cruz Biotechnology), and B7-H6 (polyclonal, 1:100, Abcam) were diluted in Renaissance Background Reducing Buffer (BioCare Medical, Pacheco, CA) and added overnight at 4°C (POU2F3) or for 45 minutes (NCAM1) or 60 minutes (all others) at room temperature. ImmPress-HRP species-specific immunoglobulin (Ig)G polymer reagents (Vector Laboratories) were used as secondary antibodies; opal fluorophores (Opal-480, 520, 570, 620, and 690, Akoya Biosciences) were used for signal detection, according to the manufacturer's protocol. Slides were counterstained with 4′,6-diamidino-2-phenylindole (DAPI) (1:1000 dilution, Invitrogen, Waltham, MA) and mounted using ProLong Diamond mountant (Invitrogen). Slide scanning and image capturing were performed on an Axio Scan.Z1 and Zen Blue software (Zeiss). Expression of NCAM1, MHC-class I, and B7-H6 was each considered positive if more than 10% of the tumor cells in an individual tumor core exhibited membrane-localized expression of the corresponding marker. The expression of ASCL1, NEUROD1, POU2F3, and YAP1 was considered positive if localized to the nucleus of tumor cells; tissues were categorized into the SCLC molecular subtypes on the basis of which transcription factor was expressed in the highest percentage of tumor cells within each individual core. Tissues were assessed by two individuals.

Fluorescent RNA In Situ Hybridization

The SCLC tumor array described previously (LC818c) was used to evaluate infiltration with the NK cells; RNA in situ hybridization for human CD49b and NCR3 (NKp30) was performed according to the manufacturer's protocol (Advanced Cell Diagnostics, Newark, CA). A subset of cases were randomly chosen for quantification analysis: $ASCL1^{POS}$ MHC-class I^{NEG}, $ASCL1^{POS}$ MHC-class I^{POS}, $NEUROD1^{POS}$, $POU2F3^{POS}$ (n = 5 tissues each), and $YAP1^{POS}$ (n = 2 tissues). A region of interest (ROI) was randomly drawn within two distinct areas of the tumor, and Zen Blue software (Zeiss) was used to count the $DAPI^{POS}$ cells within each ROI. NK cells within each ROI, identified as $CD49b^{POS}/NCR3^{POS}$ cells, were counted manually by two individuals, and the average of these counts was used to calculate the number of NK cells per 1000 $DAPI^{POS}$ cells.

Real-Time Polymerase Chain Reaction

Total RNA was isolated from tumor cells using the RNeasy Mini Kit (Qiagen, Germantown, MD). For quantitative polymerase chain reaction (PCR) analysis, RNA was reverse transcribed using the Advantage RT-for-PCR Kit (Takara Bio, Mountain View, CA), and complementary DNA was purified by the QIAquick PCR purification kit (Qiagen). All kits were used according to the manufacturer's instructions. Complementary DNA (20 ng) was amplified using TaqMan Master Mix (Thermo Fisher Scientific, Waltham, MA) or FastStart Essential DNA Probes Master Mix (Roche, Indianapolis, IN) in either an Applied Biosystems 7500 (Thermo Fisher Scientific) or a LightCycler 96 (Roche, Basel, Switzerland) instrument. The following TaqMan gene expression probes were

used (Thermo Fisher Scientific): ASCL1 (Hs00269932_m1), HLA-A (Hs01058806_g1), HLA-B (Hs00818803_g1), HLA-C (Hs00740298), HLA-E (Hs03045171_m1), ICAM1 (Hs00164932_m1), MICA (Hs00792195_m1), MICB (Hs00792952_m1), NCR3LG1 (Hs02340611_m1), NEUROD1 (Hs01922995_s1), POU2F3 (Hs00205009_m1), PVR (Hs00197846_m1), RAET1E (Hs01026642_m1), RAET1G (Hs01584111_mH), RAET1L (Hs04194671_s1), ULBP1 (Hs00360941_m1), ULBP2 (Hs00607609_mH), ULBP3 (Hs00225909_m1), YAP1 (Hs00902712_g1), and GAPDH Control Mix (4325792). Expression of each gene of interest was normalized to that of GAPDH, as follows: $2^{-[Ct(GAPDH) - Ct(gene\ of\ interest)]}$. A heatmap of log_2-transformed, normalized expression was generated using the Partek Genomics Suite analysis software (Partek, Chesterfield, MO). Data for each gene were standardized to a mean of zero and scaled to an SD of one.

Analysis of RNAseq Data From SCLC Patient Specimens

Normalized RNAseq data from 88 biopsies from a range of metastatic sites obtained from 62 patients with SCLC available from a previously published report[4] were analyzed on Partek for expression of selected genes relevant to NK activity, including ligands for NK activating and NK inhibitory receptors (*MICA*, *MICB*, *ULBP1–3*, *RAET1E*, *RAET1G*, *RAET1L*, *NCR3LG1*, *PVR*, *ICAM1*, *HLA-A*, *HLA-B*, *HLA-C*, *HLA-E*) and a 20-gene signature of NK infiltration previously reported.[17] A heatmap of expression was generated as indicated previously. Tumor tissue classifications in NE, non-NE, and the four molecular subtypes were taken directly from Lissa et al.[4]

Cytotoxicity Assays

NK cells were isolated from PBMC by using a magnetic NK Cell Isolation Kit (Miltenyi Biotech, Auburn, CA). When indicated, the NK cells were incubated with 50 ng/mL of N-803 or the molecular equivalent of 15 ng/mL of recombinant human cytokines IL-15 or IL-2 for 48 hours before the assay, and matched donor unstimulated cells were isolated on the day of the assay. At the time of the assay, target cells were harvested, washed, labeled with 10 μM calcein-AM (Invitrogen) for 20 minutes at 37°C, washed, and plated at 4 to 5 × 10^3 cells per well in 384-well flat-bottom culture plates. NK effector cells from various donors were added at effector-to-target (E:T) ratios ranging between 20:1 and 1:1 as indicated in the figure legends. After a 6-hour or 24-hour co-culture incubation as indicated, viable calcein-AM^{POS} cells were quantified using a Celigo Image Cytometer (Nexcelom Bioscience, Lawrence, MA). Percent lysis was calculated as follows: % lysis = [1 - (cell count in well of interest/tumor only average cell count)] × 100. In the case of antibody-dependent cellular cytotoxicity (ADCC) assays, cetuximab (10 ng/mL) was incubated with target cells 30 minutes prior and throughout the duration of the experiment. For Fc blocking assays, isolated NK cells were incubated with functional grade, blocking anti-CD16 monoclonal antibody (Invitrogen, clone B73.1, 25 μg/mL) for 1 hour before incubation with N-803 (50 ng/mL) for 24 hours. At the time of the assay, N-803 was washed out and anti-CD16 antibody (25 μg/mL) was refreshed for the duration of the 6-hour co-culture incubation.

Tumor Inoculation and Treatment

All animal studies were approved by the NIH Intramural Animal Care and Use Committee. Mice were maintained within guidelines provided by the Association for Assessment and Accreditation of Laboratory Animal Care in pathogen-free conditions. Eight-week-old female athymic nude (NU/NU) mice were obtained from the NCI Frederick Cancer Research Facility. Mice were injected subcutaneously in the right flank with 6×10^6 H841 cells mixed at a 1:1 ratio with Matrigel (Corning Life Sciences, Corning, NY). N-803 was administered weekly by subcutaneous injection at a dose of 1 μg beginning on day 7. Tumors were measured with a Vernier caliper two to three times per week in two perpendicular diameters. Tumor volume = (short diameter^2 × long diameter)/2.

Formalin-fixed, paraffin-embedded tissue slides from H841 tumor xenografts were stained with anti–MHC-class I (clone EMR8–5, 1:1000, Abcam) following the procedure described previously. For image quantification, four equal-sized ROIs were randomly selected per tumor section in regions without obvious signs of necrosis. Mean fluorescence intensity (MFI) for MHC-class I expression was collected for each ROI and averaged to a single MFI per individual tumor section.

Flow Cytometry

Cells were stained in 96-well flat-bottom plates using 1X phosphate-buffered saline containing 2% fetal bovine serum. All antibodies used were purchased from BioLegend (San Diego, CA), BD Biosciences, R&D Systems (Minneapolis, MN), or Thermo Fisher Scientific and used according to manufacturers' instructions. When applicable, intracellular staining was performed using a FoxP3/Transcription Factor Staining Buffer Set (eBioscience, San Diego, CA) according to the manufacturer's protocol. LIVE/DEAD Fixable Aqua Dead Cell Stain Kit (Thermo Fisher Scientific) was used to gate on live cells. All cytometry data were acquired using the Attune NxT Flow Cytometer (Thermo Fisher Scientific), and data were analyzed by FlowJo (FlowJo, Ashland, OR). For analysis from in vivo studies, tumors were weighed, mechanically dissociated, and incubated in Roswell Park Memorial Institute 1640 Medium containing 5% fetal bovine serum, 1 mg/mL collagenase types I and IV (Gibco), and 40 U/mL DNase I at 37°C for 30 minutes while shaking at a speed of 300 rpm. Subsequently, the cells were passed through a 70-μm filter to generate a single-cell suspension for staining. Spleens were crushed through a 70-μm filter, and red cell lysis was performed using ammoniumchloride-potassium lysis buffer (Gibco) on ice. For these flow analyses, cells were enumerated by 123count eBeads (Thermo Fisher Scientific) according to the manufacturer's instructions, and NK cells were defined as $CD45^{POS}CD49b^{POS}$. Fluorescently labeled antibodies used were as follows: human CD3 (clone OKT3), CD14 (clone M5E2), CD16 (clone 3G8), CD19 (clone HIB19), CD56/NCAM1 (clone HCD56), EGFR (clone AY13), NKp30 (clone P30–15), NKp44 (clone P44–8), NKp46 (clone 9E2), NKG2D (clone 1D11), perforin (clone dG9), granzyme B (clone QA18A28), MIC-A/B (clone 6D4), CD54 (clone HCD54), HLA-A/B/C (clone W6/32), and CD274 (clone 29E.2A3); murine CD45 (clone 30-F11), CD49b (clone DX5), NKG2D (clone C7), IFN-γ (clone XMG1.2), KLRG1 (clone 2F1), TIM-3 (clone RMT3–23), and PD-1 (clone RMP1–30) from BioLegend; human ULBP-2/5/6 (clone 165903, R&D Systems); and human B7-H6 (clone JAM1EW, Thermo Fisher Scientific). Unless indicated

in the figure legend, all flow analyses were assessed by gating on cells by a FSC × SSC plot followed by single cells (FSC-A × FSC-H) and then by live cells (absence of Aqua Dead Cell Stain).

Enzyme-Linked Immunosorbent Assay

For analysis from in vivo studies, blood was collected at study end point into EDTA-K tubes and plasma isolated by centrifugation. Plasma IFN-γ was assessed using the mouse IFN-γ Quantikine Enzyme-Linked Immunosorbent Assay Kit (R&D Systems) according to the manufacturer's instructions.

B7-H6 Overexpression

DMS114 and H841 cells were transfected with either a control pCMV6 or a human B7-H6 (NCR3LG1, Myc-DKK tagged)–expressing vector (Origene, Rockville, MD) using Lipofectamine 3000 (Thermo Fisher) following the manufacturer's recommendations. Then, 48 hours after the transfection, the cells were collected, assessed for B7-H6 expression by flow cytometry, and used in a flow-based cytotoxic assay. Target cells were prepared with 10 μM calcein-AM as described in earlier methods, and 1×10^4 cells per well were plated in 96-well round bottom plates. NK effector cells were added at an E:T ratio of 20:1, and after a 6-hour coincubation, samples were stained for assessment of HLA-A/B/C and B7-H6 by flow cytometry using the same antibodies described previously; in addition, to calculate % lysis, the cells were enumerated by 123count eBeads. Analyses were completed on the basis of gating on cells by FSC × SSC plots and then by calcein-AM^{HIGH} or calcein-AM^{LOW} levels followed by an assessment of surviving (calcein-AM^{HIGH}) cells for expression level of MHC-class I and B7-H6.

Generation of MHC-Class I^{LOW} Tumor Cell Lines

Generation of MHC^{LOW} tumor cells was achieved by CRISPR knockout of beta-2-microglobulin (B2M). Briefly, tumor cells were cotransfected with a recombinant TrueCut Cas9 Protein v2 and a TrueGuide Synthetic guide RNA targeting human B2M (ID number, CRISPR983706_SGM targeting the sequence GAGTAGCGCGAGCACAGCTA), by using the Lipofectamine CRISPRMAX transfection reagent. All reagents were purchased from Thermo Fisher Scientific, and assays were performed by following the manufacturer's recommended protocol. MHC-class I^{LOW} cells were flow sorted by HLA-A/B/C staining (BD, Clone G46–2.6) and expanded for cytotoxic assays.

Statistical Analyses

Data were analyzed using GraphPad Prism (GraphPad Software). Statistical differences between two sets of data were determined by a two-tailed Student's *t* test; three or more sets of data were compared by a one-way analysis of variance (ANOVA) with Tukey's multiple comparison post-tests. Analysis of tumor growth curves and killing assay assessments evaluating multiple effectors and E:T ratios simultaneously were conducted by a two-way ANOVA. Data points in graphs represent the mean ± SD. Violin plots reveal values for each individual with dashed lines indicating the median and each quartile. Asterisks indicate

statistically significant values indicated as follows: *p less than or equal to 0.05; **p less than or equal to 0.01; ***p less than or equal to 0.001, ****p less than or equal to 0.0001.

Results

NE Subtypes of SCLC Express Fewer NK Inhibitory Ligands

A lack of MHC-class I expression in SCLC is proposed to be in part responsible for the lack of response to ICB in these immunologically "cold" tumors; in contrary, it is known that NK cell activity may be improved in the absence of MHC-class I expression. Therefore, to investigate the level of MHC-class I expression in SCLC in relation to the NE versus non-NE subtypes of SCLC, a tumor tissue array consisting of 80 independent cases was co-stained for MHC-class I and a marker of the NE phenotype, NCAM1 (Fig. 1A and Supplementary Table 1). Although most of the tumors, 61 (76%), displayed an NE phenotype (NCAM1^{POS}) with a lack of MHC-class I expression, a small subset of 11 tumors (14%) were positive for both markers, with heterogeneous patterns of expression observed across cases. Non-NE (NCAM1^{NEG}) tumors were divided into two subsets as well; four tumors (5%) expressed high levels of MHC-class I, and four (5%) lacked expression of either protein (Fig. 1A and B). Overall, 65 tumors (81%) in this array lacked MHC-class I expression, most of which were NE tumors (Fig. 1B). To further address whether a relationship between the lack of MHC-class I and the molecular subtypes of SCLC exists, a serial tissue array section was stained for ASCL1, NEUROD1, POU2F3, YAP1, and MHC-class I expression. Tissues were categorized into SCLC subtypes on the basis of the predominant transcription factor observed; examples of tumors of each subtype co-stained with MHC-class I are illustrated in Figure 1C. In addition, 72 tumors (91%) were classified as NE with 58 (73%) being ASCL1^{POS}, ten (13%) NEUROD1^{POS}, and four (5%) exhibiting expression of both markers (ASCL1^{POS} NEUROD1^{POS}, A/N Mix). The remaining seven cases (9%) were non-NE tumors with five (6%) being POU2F3^{POS} and two (3%) YAP1^{POS} (Fig. 1D and Supplementary Table 1).

To evaluate the presence of NK tumor-infiltrating lymphocytes (NK-TILs) within SCLC, a subsequent tumor array section was analyzed for NK cells by RNA in situ hybridization (Fig. 1E). A total of 22 tissue sections that included tumors representing each molecular subtype and MHC expression status were chosen for the analysis. Two regions of interest within each tumor were assessed for the quantity of infiltrating NK cells relative to the number of DAPI^{POS} cells present within the evaluated region. The highest level of immune infiltration by the NK cells was observed in YAP1^{POS} tumors; importantly, the NK cells were observed within every tissue analyzed with no distinction in the quantity of NK-TIL observed within the ASCL1, NEUROD1, or POU2F3 SCLC cases or between MHC^{POS} and MHC^{NEG} tumors (Fig. 1F).

To further evaluate the presence of the NK cells and the favorability of the SCLC tumor microenvironment for NK-based therapeutic approaches, previously published RNAseq data from 88 tumor biopsies from 62 metastatic patients with SCLC were analyzed.[4] Genes chosen for evaluation included a 20-gene signature of NK cell infiltration previously published[17] and additional genes known to be involved in NK activation or inhibition. As found in Figure 1G, expression of NK activating and NK inhibitory ligands was variable

among NE and non-NE samples, apart from MHC-class I expression that was highly positive in most of the YAP1^{POS} tumors, as previously reported.[10,18] YAP1^{POS} tumors were also enriched for the NK infiltration gene signature, although expression of this signature was also observed in some of the tumors in the NE group (Fig. 1G).

To conduct preclinical studies, a panel of cell line models encompassing two from each of the four molecular subtypes of SCLC was then selected on the basis of their previously reported molecular classification.[19] Cell lines were validated for expression of ASCL1, NEUROD1, POU2F3, and YAP1 and evaluated for expression of genes relevant to NK-mediated response by quantitative reverse transcription PCR. Results further confirmed that HLA genes were increased in non-NE tumor cell lines. Although ULBP-activating genes were heterogeneous across cell lines, MIC-A/B genes were primarily expressed by YAP1^{POS} cells, and the activating ligand NCR3LG1 (B7-H6) had a trend toward higher expression in NE cell lines (Fig. 1H).

NE SCLC Cells Are Susceptible to NK-Mediated Lysis Whereas Non-NE SCLC Cells Remain Refractory

To evaluate the cytotoxicity of NK cells against SCLC, tumor cells were coincubated with effector NK cells isolated from healthy donor PBMC at an E:T ratio of 10:1. The ASCL1^{POS} cell lines, DMS79 and H69, were selected as representative of NE SCLC tumors, whereas the YAP1^{POS} cell lines, DMS114 and H841, were selected as representative of non-NE SCLC tumors. Although the NE SCLC cell lines were highly susceptible to NK-mediated lysis, the non-NE SCLC models were refractory to lysis by the NK cells (Fig. 1I). Addition of the IgG1 EGFRspecific antibody, cetuximab, to trigger ADCC was unable to overcome the resistance of non-NE, H841 cells to NK killing (Supplementary Fig. 1A), regardless of the high expression of EGFR in these cells (Supplementary Fig. 1B).

NK Cells Pretreated With the IL-15 Superagonist N-803 Effectively Lyse SCLC Cell Lines of All Variant Subtypes

Cytokine-activated NK cells were then evaluated for their lytic activity against SCLC cell lines. Recombinant human IL-2 (rhIL-2) and IL-15 (rhIL-15) along with the IL-15 superagonist, N-803, were used to activate the NK cells before assessing their functional activity. Healthy donor NK cells were incubated in culture with equimolar concentration of each cytokine for 48 hours, washed, and used as effector cells against SCLC cells. As illustrated in Figure 2A, pretreatment of the NK cells with each cytokine significantly enhanced the ability of the NK cells to lyse NE (ASCL1^{POS}) and non-NE (YAP1^{POS}) cells. Although the efficacy of the three cytokines was similar in vitro at the dose evaluated, N-803 was selected for further evaluation in this study owing to its suitability for clinical use. Although IL-2 has the disadvantage of expanding regulatory T cells and IL-15 has a very short half-life in vivo, N-803 was found to have higher biostability with fewer dose-limiting toxicities than IL-15 in vivo, making it a more suitable choice for a clinical reagent.[16,20] To evaluate the contribution of the IgG1 Fc portion of N-803 to the activation of the NK cells in vitro, including to rule out any ADCC effect, NK cells from healthy donors were incubated with N-803 in the presence of a CD16 Fc receptor blocking antibody and used in a cytotoxic assay in the presence of CD16 Fc receptor blockade. As found in Supplementary

Figure 1C, there was only a minimal change in tumor lysis in assays blocking the CD16 Fc receptor indicating that in vitro, N-803 can mediate NK cell activation independently of its Fc component and that the IgG1 Fc fraction does not contribute to lysis by ADCC. In subsequent experiments, healthy donor NK cells pretreated with N-803 were found to efficiently lyse SCLC cells across the four molecular subtypes, at all E:T ratios evaluated (Fig. 2B and C). As variation in the lytic capacity of the NK cells isolated from different donors is known to exist, lysis of all eight SCLC models was also assessed using matched NK cells (untreated or pretreated with N-803 for 48 h) purified from PBMC from multiple healthy donors. In the case of all normal donor-derived NK cells, pretreatment with N-803 significantly and markedly enhanced the lysis of all SCLC cell lines evaluated, including NE and non-NE models (Fig. 2D).

N-803 Provides Antitumor Efficacy In Vivo by Improving Activation of Murine NK Cells

To evaluate the efficacy of N-803 treatment in vivo, a xenograft model of the H841 SCLC cell line was used. This model was chosen owing to its highly NK-resistant character to validate the ability of N-803 to improve the lytic effect of NK cells in vivo even against the most NK-resistant tumors. H841 cells were implanted (subcutaneously) in the flank of athymic nude mice, which are devoid of T and B cells but possess normal levels of NK cells. Starting on day 7 post-tumor implantation, mice in the treatment group received a weekly dose of 1 μg N-803 (subcutaneously) for a total of four doses (Fig. 3A). N-803–treated mice exhibited significantly improved tumor control compared with untreated mice, as observed in the average tumor volume (Fig. 3B) and the tumor growth curves of individual mice (Fig. 3C). Similar results were observed in an independent experiment (Supplementary Fig. 2A and B). To evaluate the effect of N-803 on murine NK cells, tumors and spleens were collected 48 hours after the last dose of N-803 and evaluated by flow cytometry. Although the spleens of the treated mice did not exhibit an overall change in the total number of NK cells per spleen, N-803–treated mice had a significantly higher number of NKG2D^{POS} NK cells compared with the controls, indicative of a more activated population of NK cells (Fig. 3D). In addition, there was a significantly higher number of multifunctional NK cells in the spleens of N-803–treated mice, which produced IFN-γ and granzyme B, indicative of a more lytic NK phenotype (Fig. 3D). Analysis of tumor infiltrates revealed significantly higher numbers of murine NK cells infiltrating the N-803–treated tumors and significantly higher numbers of NKG2D^{POS} and NK-TIL capable of producing both IFN-g and granzyme B in the N-803–treated tumors, compared with the controls (Fig. 3E). Comparable numbers of NK cells expressing inhibitory receptors were observed within the tumors of untreated and N-803–treated mice (Supplementary Fig. 2C). A small increase in TIM-3^{POS} or PD-1^{POS} but not TIM-3^{POS}/PD-1^{POS} double-positive NKs was observed in the spleens of treated mice (Supplementary Fig. 2D); further analysis would be needed to determine if this represents increased activation or exhaustion of these cells. To assess the level of circulating IFN-γ in animals untreated or treated with N-803, blood was collected 48 hours after the last treatment and plasma was isolated for evaluation by enzyme-linked immunosorbent assay; results indicated that N-803–treated mice exhibited higher levels of murine IFN-γ in circulation than the untreated mice (Fig. 3F). As high levels of IFN-γ are known to affect tumor expression of MHC-class I, tumors remaining at the end of study were stained to assess any modifications in MHC-class I expression. The

H841 model is known to express basal levels of MHC-class I; however, it was observed that the MFI of MHC-class I increased by twofold or greater in N-803– treated mice (Fig. 3G and H). This finding suggests that the immunogenicity of SCLC tumors may be improved for T-cell–based therapeutics after N-803 administration; future studies should evaluate the effectiveness of a sequential combination therapy with N-803 followed by immunotherapeutic agents that rely on T-cell activity, including ICB. Taken together, these data revealed that NK cells become more activated in vivo by N-803, can better traffic to the site of the tumor, impart improved antitumor efficacy, and produce high levels of IFN-γ, which, in turn, create an “immune hot” tumor microenvironment.

N-803–Treated NK Cells Could Prime Tumor Cells for Additional Immunotherapy Modalities

To further evaluate how SCLC cancer cells may be affected by exposure to soluble factors secreted by NK cells stimulated with N-803, a panel of key NK activating and NK inhibitory ligands were measured by flow cytometry in tumor cells cultured in the presence of either standard culture media or conditioned media from NK cells treated with N-803. Among NK activating ligands, it was observed that MIC-A/B were expressed exclusively by YAP1^{POS} cell lines, whereas ULBP-2/5/6 were expressed throughout most of the cell lines, except in H82 cells. B7-H6, the cognate ligand for NKp30 activation on the NK cells, and CD54 (ICAM1) were both found at higher levels on the NE cells. Importantly, exposure to culture supernatant from the NK cells treated with N-803 did not induce many changes in the expression of NK activating ligands, apart from CD54, which was markedly up-regulated in all but the YAP1^{POS} cell lines, H841 and DMS114 (Fig. 4A and B). Regarding NK inhibitory ligands, PD-L1 expression was minimal or negative at baseline but increased in most cell lines after exposure to culture supernatant from N-803–activated NK cells, with exceptions being DMS114 and H524 cells (Fig. 4C and D). Furthermore, although all cell lines express MHC-class I (HLA-A/B/C) at the protein level, those of the non-NE subtypes expressed logarithmically higher levels (Fig. 4C); on the basis of this observation, the MFI of HLA-A/B/C was quantified rather than the percentage of tumor cells (Fig. 4D). Interestingly, conditioned media from the NK cells treated with N-803 caused significant increases in the expression of MHC-class I in all cell lines, regardless of their molecular subtype. Similarly, NE and non-NE cells exposed to culture supernatants from the NK cells activated by either N-803, rhIL-15, or rhIL-2 for 48 hours had comparable increases in the MFI of HLA-A/B/C above that of the untreated cell lines (Fig. 4E). Consistent with in vivo observations, these data indicated that soluble factors released by NK cells after treatment with N-803 could increase the expression of MHC-class I even in SCLC tumor cells of the NE subtype, making them potentially susceptible to T-cell centric therapies that require antigen presentation in the context of MHC-class I, such as ICB, adoptive T-cell therapies, and cancer vaccines.

Impact of N-803 on NK Cells Derived From Healthy Donors and Patients With SCLC

The effect of N-803 on the NK cells was evaluated by flow cytometry analysis for expression of NK activating receptors and cytolytic molecules. As found in Figure 5A for multiple matched healthy donor-derived NK cells, N-803 treatment of the NK cells increased the surface expression of all four NK activating receptors, NKp30, NKp44, NKp46, and NKG2D, in most of the donors analyzed, with the most prominent and

consistent increase observed with NKp30 (Fig. 5A and Supplementary Fig. 3A). Cytolytic perforin and granzyme B levels were high in most of the untreated, healthy donor NK cells, with only minor increases induced by N-803 stimulation in some of the donors (Fig. 5A).

To investigate whether N-803 could also effectively activate NK cells derived from patients with SCLC, PBMC obtained from three patients with SCLC previously treated with various lines of therapy, including chemotherapy, were exposed to N-803 for 48 hours and evaluated for NK cell markers and expression of cytolytic molecules in the NK cells, as surrogate markers for cytotoxicity. As a comparison, PBMCs from the three healthy donors were used. Individual subsets of NK cells were evaluated,[21] including the highly cytotoxic $CD56^{DIM}$ $CD16^{POS}$ cells, cytokine-producing $CD56^{BRIGHT}$ $CD16^{NEG}$ cells, and more immature precursor $CD56^{BRIGHT}$ $CD16^{POS}$ cells (Fig. 5B, left panel, and Supplementary Fig. 3B). N-803 treatment of PBMC similarly increased the number of $CD56^{BRIGHT}$ cells (both $CD16^{NEG}$ and $CD16^{POS}$ fractions) in healthy donors and patients as found in Figure 5B for representative samples, and for all individuals evaluated in Figure 5C. To further assess the cytolytic potential of NK cells within each subset, perforin and granzyme B were measured. The most cytolytic cells ($CD56^{DIM}$ $CD16^{POS}$) had a consistent increase in the percent of $perforin^{POS}$ or granzyme B^{POS} cells and the MFI for each molecule after treatment with N-803 in all patients and healthy donors evaluated (Fig. 5D, left panels). Increases in perforin and granzyme B were also observed in the $CD56^{BRIGHT}$ NK subsets (Fig. 5D, central and right panels), both with healthy donors and SCLC patient-derived NK cells. Taken together, these data revealed that N-803 treatment exerts similar effects on NK cells derived from healthy donors and patients with SCLC, suggesting that N-803 treatment is likely to increase the lytic potential of NK cells from the patients with SCLC.

The Role of the NKp30-B7-H6 Axis Activation in NK-Mediated Lysis of SCLC Cells

NKp30 binds to B7-H6 (NCR3LG1) to activate the NK cells,[22] and recent literature suggests a particular importance of this interaction in the context of cancer.[23] To investigate whether expression of B7-H6 could be of relevance in the context of NK-mediated lysis of SCLC, B7-H6 was overexpressed on the surface of the non-NE (DMS114 and H841) cells before performing NK lysis assays. By increasing the surface expression of B7-H6, both non-NE SCLC lines became significantly more susceptible to lysis by healthy donor NK cells (Fig. 6A). In addition, tumor cells that survived the cytolytic effect of the NK cells were further assessed by flow cytometry for their expression of B7-H6 and MHC-class I. Results revealed that most B7-H6–expressing tumor cells were eliminated (Fig. 6B and C and Supplementary Fig. 4A and B) whereas all surviving cells continued to express MHC-class I (Fig. 6D). As the expression of MHC-class I remained unchanged, beta-2-microglobulin (B2M) was knocked out in DMS114 and H841 cells using CRISPR/ Cas9 technology in an attempt to further understand the direct contribution of MHC-class I to their NK-resistant phenotype. In the absence of B2M, MHC-class I molecules are no longer stably expressed on the tumor cell surface (Supplementary Fig. 4C); however, despite the loss of MHC-class I expression, lysis with NK or NK cells pretreated with N-803 did not improve in the non-NE, DMS114, or H841 B2M KO cells (Fig. 6E). Collectively, these data suggested that regardless of the level of expression of inhibitory MHC-class I molecules, improving the interaction between

NKp30 and B7-H6 enables the cytotoxic activity of the NK cells leading to lysis of the highly resistant, non-NE SCLC cells.

To evaluate the expression of B7-H6 protein in tumor tissues, a tissue array of SCLC tumors was co-stained for B7-H6 along with NCAM1 as a marker of NE phenotype (Fig. 6F and Supplementary Table 1). As expected, most cases presented as NE tumors ($NCAM1^{POS}$, 69 of 79, 88%); within these tumors, 37 of 69 (54%) were also positive for B7-H6 (Fig. 6F and G). The high percentage of SCLC tumors which express B7-H6 and the improvements in NK-cell susceptibility observed with increased expression of the tumor ligand suggested that the B7-H6/NKp30 axis may be useful to exploit therapeutically in the context of SCLC.

Discussion

This work describes an NK-cell–based immunotherapy option for the treatment of all molecular subtypes of SCLC. The data presented reveal that NK cells activated by the IL-15 superagonist, N-803, effectively lyse SCLC tumor cells across all variant subtypes and that administration of N-803 in vivo enhances tumor infiltration with activated and cytotoxic NK cells, leading to antitumor efficacy against SCLC xenografts.

Despite the success of ICB therapies for the treatment of several cancers, immunotherapy has so far provided limited clinical benefit in SCLC. The PD-L1 inhibitors, durvalumab[24] and atezolizumab,[25] used in combination with platinum-etoposide chemotherapy, are currently approved for the first-line treatment of extensive-stage SCLC. In this setting, addition of anti–PD-L1 to chemotherapy in several randomized clinical studies has resulted in an improvement in overall survival (OS) of approximately 2 months compared with chemotherapy alone. This modest clinical benefit of ICB in SCLC has been attributed to the presence of an unfavorable tumor microenvironment mainly characterized by low T-cell infiltration and low expression of MHC-class I, with exception of a small percentage of tumors in the non-NE molecular subtypes.[6,7,26] In further efforts to identify a predictive biomarker to delineate who will benefit from ICB, a recent study also found that tumors from patients with relapsed SCLC who benefited from ICB therapy had increased levels of Notch pathway genes and low NE differentiation.[27] It is yet to be determined whether clinical practice in SCLC will move toward stratifying patients into groups on the basis of molecular subtype of their tumor before therapy. In addition, SCLC is a heterogeneous disease where different molecular subtypes could be found within a single tumor, particularly after tumor relapse.[5] In light of these limitations, an alternative form of immunotherapy outside of ICB was explored here which may provide benefit to most of the patients with SCLC, including those with immunologically cold tumors lacking MHC expression.

The loss of MHC-class I in NE SCLC has been attributed to epigenetic mechanisms involving the transcriptional repression of MHC-class I promoters by the polycomb repressive complex 2 (PRC2), an effect that can be reversed by pharmacologic inhibition of EZH2.[28] In agreement with previous studies,[29] this study reveals the lack of MHC-class I protein expression in 81% of SCLC in a tumor tissue microarray, most (76%) corresponding to NE tumors. Subtype analysis also reveals that, although a small sample size, $YAP1^{POS}$

tumors exhibit high MHC expression whereas most of the tumors within the ASCL1, NEUROD1, and POU2F3 subtypes lack MHC-class I protein expression. The remarkable lack of expression of MHC-class I in SCLC suggests that NK-therapeutic approaches may be more suited for this disease. In this study, the presence of NK-TIL was observed in tumor tissues from patients encompassing each molecular subtype of SCLC. RNAseq analysis in a cohort of metastatic SCLC tumors from 62 individual patients similarly indicated that both MHC expression and genes indicative of an NK signature are highest in the non-NE YAP1^{POS} tumors, although tumors in the NE subtypes also present with variable levels of MHC-class I and NK gene-associated signatures. Although the literature supports that YAP1^{POS} SCLC tumors are the most immune infiltrated overall, our results differ from a previous report that described the highest NK score within POU2F3^{POS} SCLC tumors.[30] These differences may be attributable to differences in the patient populations as the prior study evaluated primary SCLC samples and this study metastatic samples. Future studies should be conducted to evaluate samples from individuals taken at multiple time points from the primary versus metastatic sites to address these distinctions observed.

A few studies have interrogated the potential role for NK cells in SCLC tumor control. For example, a study using a genetic engineered mouse model of SCLC revealed that although the depletion of CD8^{POS} T cells had no effect on metastatic dissemination of SCLC, depletion of the NK cells resulted in increased metastatic spread to various organs, suggesting that NK cells play a critical role in SCLC immunosurveillance and tumor dissemination control.[30] Another study, however, proposed that despite the lack of MHC-class I expression, SCLC tumors also may evade NK cell surveillance by down-regulating the expression of NK activating ligands, specifically MICA/B, which were found to be expressed at lower levels in NE versus non-NE tumors.[31] Using the NK cells isolated from multiple healthy donors, this study describes that NK cells can lyse SCLC tumor cells of the NE, ASCL1, and NEUROD1 subtypes; however, the lytic effect was markedly and significantly enhanced by pretreatment of the NK cells with N-803, an effect that was extended to all SCLC models, including those of the non-NE, POU2F3, and YAP1 subtypes, which were also efficiently lysed by the N-803–treated NK cells. The utilization of chemotherapy as standard of care in all treatment regimens for SCLC implies that the quality of patient NK cells may be inferior to that of healthy donors. To address this concern, PBMC from three patients with SCLC previously treated with various chemotherapies were evaluated for their response to N-803. Paralleling results observed in healthy donor PBMC, the composition of the NK cells from the patients with SCLC shifted such that CD56^{BRIGHT} NK cells expanded. The literature suggests that the CD56^{BRIGHT} NK cells are capable of producing high levels of IFN-γ[21,32]; therefore, these changes in subsets imply that NK cells from patients with SCLC or healthy donors may have improved antitumor activity by IFN-γ–mediated mechanisms. Furthermore, all subsets of the NK cells had increased levels of cytolytic proteins, perforin, and granzyme B, in response to N-803. These findings suggest that as found with the healthy donors, NK cells from the patients with SCLC would exhibit elevated lytic capacity toward tumor cells.

N-803 is a clinical-stage, IL-15 superagonist that enhances the biological activity of IL-15 in vivo and was found in multiple preclinical studies to promote the activation of antigen-specific T cells and NK cells above the level observed with recombinant IL-15, resulting

in improved antitumor effects in murine models of cancer.[16,20] N-803 was found to have promising clinical activity with an acceptable safety profile; a randomized phase 1b study of N-803 in combination with nivolumab in previously treated patients with stage IIIB or IV NSCLC revealed objective responses in six of 21 (29%) patients, including in patients with ICB refractory disease.[14] Multiple clinical studies are currently ongoing to evaluate N-803 in combination with ICB or other immune-based therapies in patients with various types of carcinomas. In vitro data with multiple healthy donor NK cells presented here revealed that N-803 consistently increases the expression of the NK activating receptors, NKp30, NKp44, NKp46, and NKG2D on the surface of the NK cells, with the most prominent increase observed in NKp30. In vivo, analysis of tumor infiltrates in a murine model of SCLC revealed significantly higher numbers of multifunctional, activated NK cells, as denoted by higher number of NKG2D-positive NK cells that were also positive for IFN-g and granzyme B, in spleens and tumors of mice treated with N-803. Furthermore, the data revealed that N-803 primes a tumor microenvironment higher in IFN-γ; although residual in vivo tumors maintained the same expression of B7-H6 (data not shown), these tumors exhibited a significant increase in MHC-class I expression in response to the changing microenvironment. Congruously, conditioned media from N-803–stimulated NK cells caused up-regulation of the expression of immune molecules such as MHC-class I, the adhesion molecule CD54, and PD-L1 in vitro as well. In the future, it will be of interest to further evaluate combination or sequential therapeutic regimens in which N-803 therapy is used as a primary treatment in vivo or ex vivo, providing antitumor efficacy while also priming any remaining tumor cells for subsequent T-cell centric therapy such as ICB.

In an effort to understand the innate differences in the susceptibility of NE versus non-NE SCLC, specifically to NK-mediated lysis, this study found that the expression of B7-H6, the ligand for NKp30, and not the lack of MHC-class I is a major requirement for adequate NK-mediated lysis of SCLC cells. This conclusion derived from data from B7-H6 overexpression experiments where increasing B7-H6 expression in MHC-class I–high, non-NE cells resulted in markedly and significantly enhanced lysis by normal NK cells. In addition, down-regulating the expression of MHC-class I by ablation of B2M in MHC-class I–high tumor cells was unable to overcome the resistance to NK-mediated lysis, thus supporting the idea that the NKp30/B7-H6 interaction is at the center of the mechanism of lysis of SCLC tumor cells by innate NK effector cells. Although surely not the only required interaction for efficacy of the NK cells, these data support the idea that tumor expression of B7-H6 may be a useful tool to evaluate which patients may benefit from NK-centric therapeutics. Finally, an inverse relationship between the NE tumor phenotype and high levels of MHC expression was consistently observed. It would be prudent to evaluate whether this relationship exists in other tumors of NE origin and whether an initial NK-based therapy could be beneficial in this context as well.

Novel and more effective therapeutic approaches for the treatment of SCLC are urgently needed. This study highlights the potential of a novel immune-based intervention using an NK- and cytokine-based therapeutic option for the treatment of SCLC. Although the IL-15 superagonist, N-803, could be administered systemically to enable the activation of endogenous NK cells, N-803 could also be used to activate NK cells ex vivo before being infused back to patients in an autologous, adoptive NK cell transfer setting.

More importantly, the findings presented here suggest that N-803 may provide clinical benefit to most patients with SCLC across all molecular variants, including those with immunologically cold tumors lacking MHC-class I expression.

Supplementary Material

Refer to Web version on PubMed Central for supplementary material.

Acknowledgments

The authors thank Debra Weingarten for her editorial assistance in the preparation of the manuscript. This work was supported by the Intramural Research Program of the Center for Cancer Research, National Cancer Institute (NCI), National Institutes of Health (NIH), and through a Cooperative Research and Development Agreement (CRADA) between the NCI/NIH and ImmunityBio, Inc.

References

1. Rudin CM, Brambilla E, Faivre-Finn C, Sage J. Small-celllung cancer. Nat Rev Dis Primers. 2021;7:3. [PubMed: 33446664]
2. Rudin CM, Poirier JT, Byers LA, et al. Molecular subtypes of small cell lung cancer: a synthesis of human and mouse model data. Nat Rev Cancer. 2019;19:289–297. [PubMed: 30926931]
3. Ireland AS, Micinski AM, Kastner DW, et al. MYC drives temporal evolution of small cell lung cancer subtypes by reprogramming neuroendocrine fate. Cancer Cell. 2020;38:60–78.e12.
4. Lissa D, Takahashi N, Desai P, et al. Heterogeneity of neuroendocrine transcriptional states in metastatic small cell lung cancers and patient-derived models. Nat Commun. 2022;13:2023. [PubMed: 35440132]
5. Stewart CA, Gay CM, Xi Y, et al. Single-cell analysesreveal increased intratumoral heterogeneity after the onset of therapy resistance in small-cell lung cancer. Nat Cancer. 2020;1:423–436. [PubMed: 33521652]
6. Gay CM, Stewart CA, Park EM, et al. Patterns of transcription factor programs and immune pathway activation define four major subtypes of SCLC with distinct therapeutic vulnerabilities. Cancer Cell. 2021;39:346–360.e347.
7. Plaja A, Moran T, Carcereny E, et al. Small-cell lung cancer long-term survivor patients: how to find a needle in a haystack? Int J Mol Sci. 2021;22:13508.
8. Esposito G, Palumbo G, Carillio G, et al. Immunotherapyin small cell lung cancer. Cancers (Basel). 2020;12:2522. [PubMed: 32899891]
9. Dora D, Rivard C, Yu H, et al. . Neuroendocrine subtypes of small cell lung cancer differ in terms of immune microenvironment and checkpoint molecule distribution. Mol Oncol. 2020;14:1947–1965. [PubMed: 32506804]
10. Owonikoko TK, Dwivedi B, Chen Z, et al. YAP1 expression in SCLC defines a distinct subtype with T-cell-inflamed phenotype. J Thorac Oncol. 2021;16:464–476. [PubMed: 33248321]
11. Abel AM, Yang C, Thakar MS, Malarkannan S. Natural killer cells: development, maturation, and clinical utilization. Front Immunol. 2018;9:1869. [PubMed: 30150991]
12. Paul S, Lal G. The molecular mechanism of natural killer cells function and its importance in cancer immunotherapy. Front Immunol. 2017;8:1124. [PubMed: 28955340]
13. Waldmann TA. The shared and contrasting roles of IL2 and IL15 in the life and death of normal and neoplastic lymphocytes: implications for cancer therapy. Cancer Immunol Res. 2015;3:219–227. [PubMed: 25736261]
14. Wrangle JM, Velcheti V, Patel MR, et al. ALT-803, an IL-15 superagonist, in combination with nivolumab in patients with metastatic non-small cell lung cancer: a nonrandomised, open-label, phase 1b trial. Lancet Oncol. 2018;19:694–704. [PubMed: 29628312]

15. Liu B, Kong L, Han K, et al. A novel fusion of ALT-803 (interleukin (IL)-15 superagonist) with an antibody demonstrates antigen-specific antitumor responses. J Biol Chem. 2016;291:23869–23881. [PubMed: 27650494]
16. Kim PS, Kwilas AR, Xu W, et al. IL-15 superagonist/IL-15RalphaSushi-Fc fusion complex (IL-15SA/IL-15RalphaSu-Fc; ALT-803) markedly enhances specific subpopulations of NK and memory CD8þ Tcells, and mediates potent anti-tumor activity against murine breast and colon carcinomas. Oncotarget. 2016;7:16130–16145.
17. Cursons J, Souza-Fonseca-Guimaraes F, Foroutan M,et al. A gene signature predicting natural killer cell infiltration and improved survival in melanoma patients. Cancer Immunol Res. 2019;7:1162–1174. [PubMed: 31088844]
18. Cai L, Liu H, Huang F, et al. Cell-autonomous immune gene expression is repressed in pulmonary neuroendocrine cells and small cell lung cancer. Commun Biol. 2021;4:314. [PubMed: 33750914]
19. Tlemsani C, Pongor L, Elloumi F, et al. SCLC-CellMiner: are source for small cell lung cancer cell line genomics and pharmacology based on genomic signatures. Cell Rep. 2020;33:108296.
20. Rhode PR, Egan JO, Xu W, et al. Comparison of the superagonist complex, ALT-803, to IL15 as cancer immunotherapeutics in animal models. Cancer Immunol Res. 2016;4:49–60. [PubMed: 26511282]
21. Cooper MA, Fehniger TA, Caligiuri MA. The biology of human natural killer-cell subsets. Trends Immunol. 2001;22:633–640. [PubMed: 11698225]
22. Brandt CS, Baratin M, Yi EC, et al. The B7 family memberB7-H6 is a tumor cell ligand for the activating natural killer cell receptor NKp30 in humans. J Exp Med. 2009;206:1495–1503. [PubMed: 19528259]
23. Thomas PL, Groves SM, Zhang YK, et al. Beyond programmed death-ligand 1: B7-H6 emerges as a potential immunotherapy target in SCLC. J Thorac Oncol. 2021;16:1211–1223. [PubMed: 33839362]
24. Goldman JW, Dvorkin M, Chen Y, et al. Durvalumab, withor without tremelimumab, plus platinum-etoposide versus platinum-etoposide alone in first-line treatment of extensive-stage small-cell lung cancer (CASPIAN): updated results from a randomised, controlled, open-label, phase 3 trial. Lancet Oncol. 2021;22:51–65. [PubMed: 33285097]
25. Horn L, Mansfield AS, Szczesna A, et al. First-line atezolizumab plus chemotherapy in extensive-stage small-cell lung cancer. N Engl J Med. 2018;379:2220–2229. [PubMed: 30280641]
26. Remon J, Aldea M, Besse B, et al. Small cell lung cancer: a slightly less orphan disease after immunotherapy. Ann Oncol. 2021;32:698–709. [PubMed: 33737119]
27. Roper N, Velez MJ, Chiappori A, et al. Notch signalling and efficacy of PD-1/PD-L1 blockade in relapsed small cell lung cancer. Nat Commun. 2021;12:3880. [PubMed: 34162872]
28. Burr ML, Sparbier CE, Chan KL, et al. An evolutionarilyconserved function of Polycomb silences the MHC class I antigen presentation pathway and enables immune evasion in cancer. Cancer Cell. 2019;36:385–401.e388.
29. Mahadevan NR, Knelson EH, Wolff JO, et al. Intrinsic immunogenicity of small cell lung carcinoma revealed by its cellular plasticity. Cancer Discov. 2021;11:1952–1969. [PubMed: 33707236]
30. Best SA, Hess JB, Souza-Fonseca-Guimaraes F, et al. Harnessing natural killer immunity in metastatic SCLC. J Thorac Oncol. 2020;15:1507–1521. [PubMed: 32470639]
31. Zhu M, Huang Y, Bender ME, et al. Evasion of innate immunity contributes to small cell lung cancer progression and metastasis. Cancer Res. 2021;81:1813–1826. [PubMed: 33495232]
32. Wagner JA, Rosario M, Romee R, et al. . CD56bright NK cells exhibit potent antitumor responses following IL-15 priming. J Clin Invest. 2017;127:4042–4058. [PubMed: 28972539]

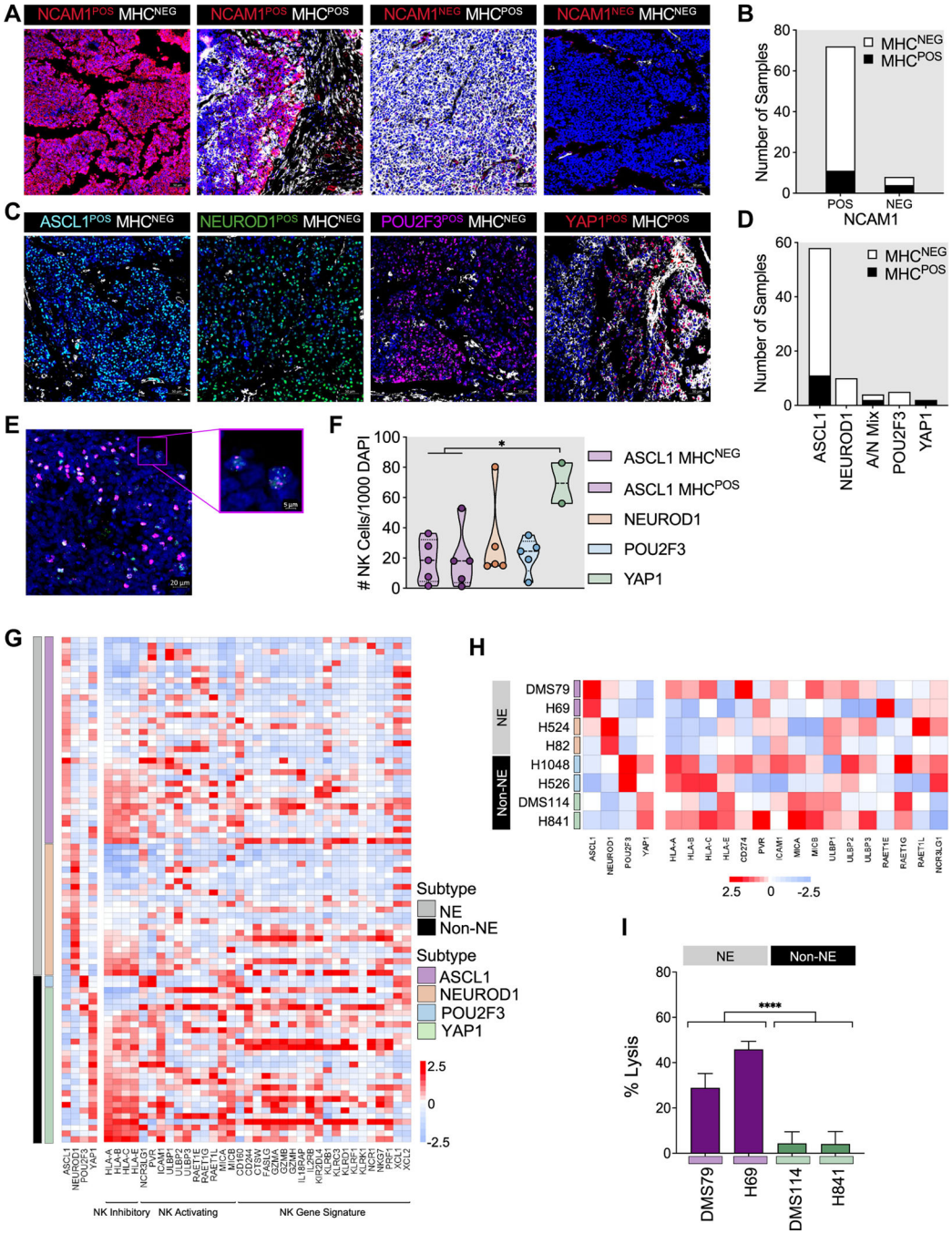

Figure 1.

Neuroendocrine SCLC express fewer factors that are inhibitory to NK cells. (*A*) Immunofluorescent staining of NCAM1 and MHC-class I proteins in SCLC tissues of a tumor microarray (NCAM1 = red, MHC-class I = white, DAPI = blue). Images representing tumor cases that are POS for NCAM1 and NEG for MHC-class I; double POS for NCAM1 and MHC-class I; NCAM1 NEG/MHC-class I POS; and double NEG for NCAM1 and MHC-class I. (*B*) Quantification of 80 SCLC tumors scored based on positivity for NCAM1 and MHC-class I expression. (*C*) Immunofluorescent staining of ASCL1, NEUROD1,

POU2F3, YAP1, and MHC-class I in SCLC tissues of a tumor microarray (ASCL1 = turquoise, NEUROD1 = green, POU2F3 = pink, YAP1 = red, MHC-class I = white, DAPI = blue). Images representing a tumor classified as each of the four subtypes of SCLC. (*D*) Quantification of 79 evaluable tumors based on the predominant transcription factor expression and MHC-class I within each case. (*E*) SCLC tissues of a tumor microarray were analyzed by RNA in situ hybridization for the presence of NK cells. Representative image depicting RNA in situ hybridization staining of CD49b mRNA (pink) and NCR3 mRNA (NKp30, green). (*F*) Quantification displays the number of NK cells per 1000 $DAPI^{POS}$ cells within a standardized ROI; analysis completed on $ASCL1^{POS}$ MHC-class I^{NEG}, $ASCL1^{POS}$ MHC-class I^{POS}, $NEUROD1^{POS}$, $POU2F3^{POS}$ (n = 5 tissues each), and $YAP1^{POS}$ (n = 2 tissues). *p < 0.05 by one-way ANOVA with Tukey's multiple comparison post-test. (*G*) Heatmap expression of ASCL1, NEUROD1, POU2F3, YAP1, and genes relevant to NK activity in 88 SCLC tumor biopsies obtained from 62 patients with metastatic SCLC previously analyzed by RNAseq analysis[4] (NE = grey, non-NE = black, ASCL1 = purple, NEUROD1 = orange, POU2F3 = blue, YAP1 = green). (*H*) Heatmap of expression of selected NK activating and NK inhibitory ligand genes as determined by quantitative reverse transcription PCR across a panel of SCLC cell lines (NE = neuroendocrine; non-NE = non-neuroendocrine). Values illustrated correspond to $\log_2$-transformed gene expression relative to the control gene GAPDH in each cell line. (*I*) Neuroendocrine (DMS79, H69) and non-neuroendocrine (DMS114, H841) SCLC cells were assayed for susceptibility to NK cells at an E:Tratio of 10:1 in a 24-hour assay. ****$p < 0.0001$ comparing NE versus non-NE by unpaired *t* test. Data illustrated are representative of n = 8 healthy NK donors. #, number; ANOVA, analysis of variance; DAPI, ′,6-diamidino-2-phenylindole; E:T, effector-to-target; NE, neuroendocrine; NEG, negative; NK, natural killer; PCR, polymerase chain reaction; POS, positive; ROI, region of interest.

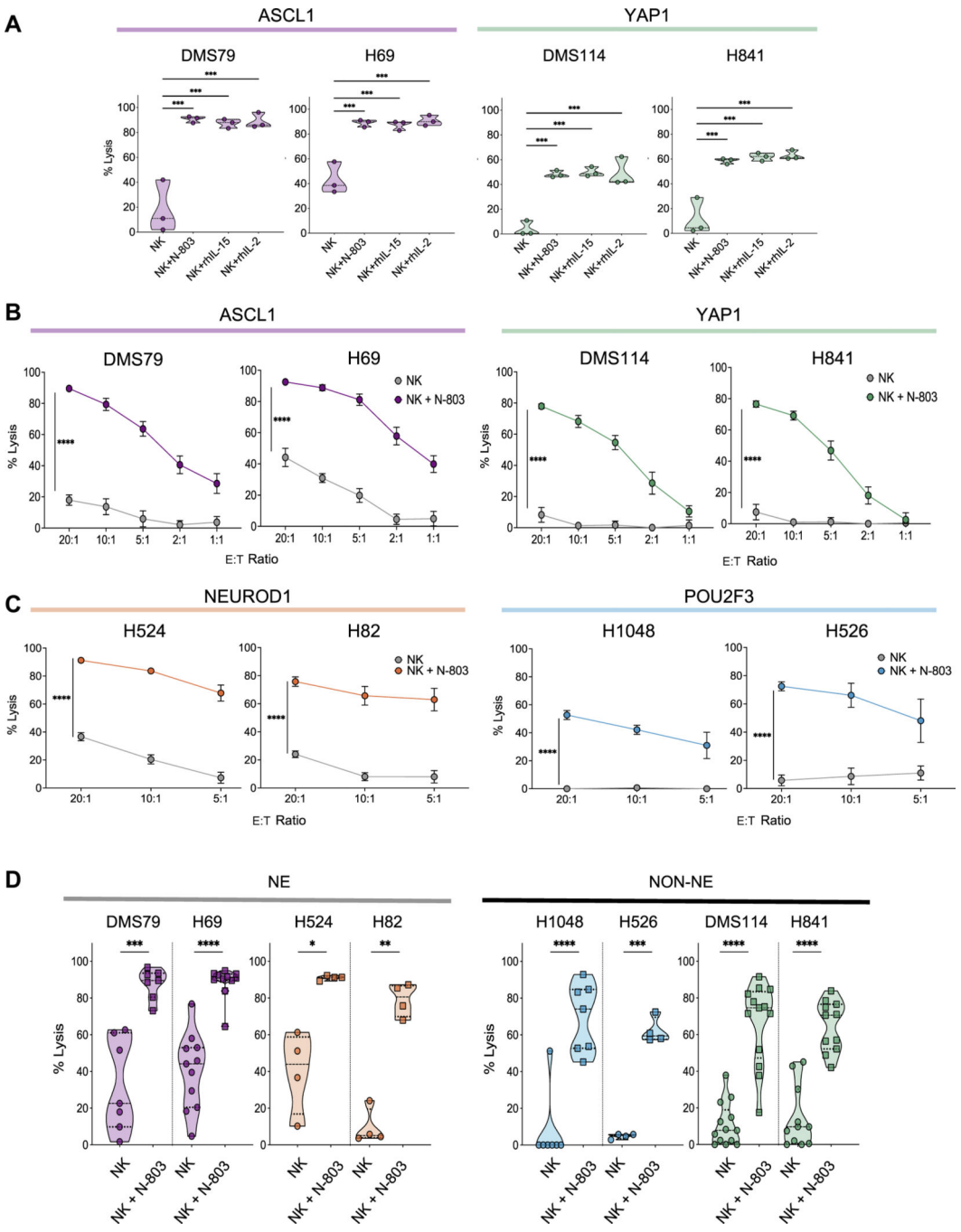

Figure 2.

NK cells pretreated with N-803 mediate tumor lysis of cell lines spanning across all subtypes of SCLC. (*A*) Percentage lysis observed using matched donor NK cells treated with either 50 ng/mL N-803, 15 ng/mL rhIL-15, or 15 ng/mL rhIL-2 for 48 hours before cytotoxicity assay. Lysis assay was carried out at an E:T ratio of 10:1 for a duration of 6 hours; unstimulated NK cells from the same donors were used as controls. Each data point represents % lysis from individual donors (n = 3). ***$p < 0.001$ by one-way ANOVA. (*B, C*) Six-hour NK lysis assay of indicated cell lines using matched donor NK cells either freshly

isolated or preincubated with 50 ng/mL N-803 for 48 hours before the cytotoxic assay, at the indicated E:T ratios. ****$p < 0.0001$ by two-way ANOVA. (*D*) Percent lysis achieved with NK cells versus NK cells pretreated with N-803 from multiple matched donors, across all cell lines and using an E:T ratio of 20:1. Each data point indicates % lysis from an individual donor used in experiments. *$p < 0.05$, **$p < 0.01$, ***$p < 0.001$, ****$p < 0.0001$ comparing average % lysis with NK (circles) versus N-803 pretreated NK (squares) effectors for each target cell line in a paired *t* test. ANOVA, analysis of variance; E:T, effector-to-target; NK, natural killer; rhIL, recombinant human interleukin.

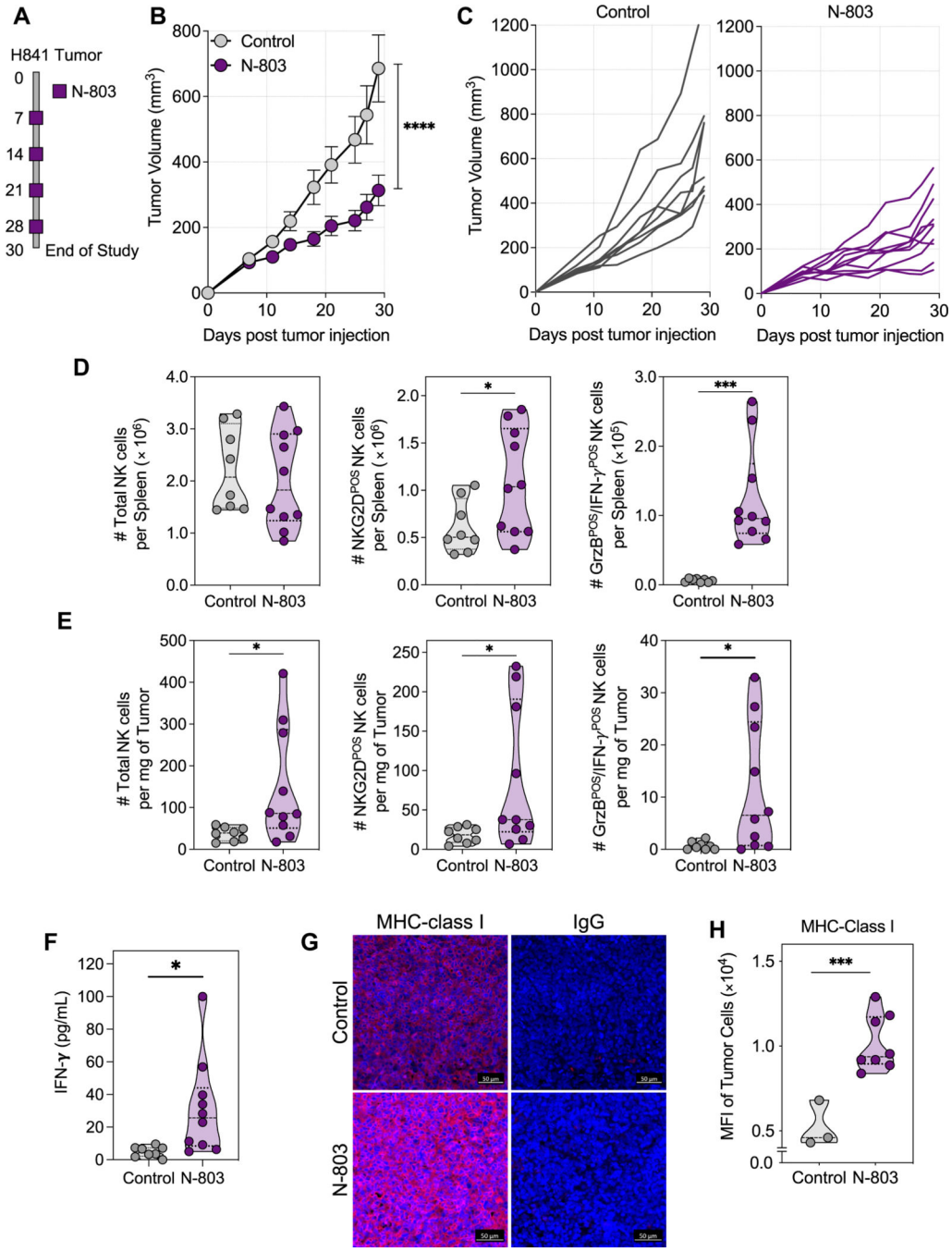

Figure 3.

N-803 improves NK-cell activation and tumor infiltration with NK cells in vivo resulting in antitumor control. (*A*) Schema of tumor and N-803 administration in vivo. (*B*) Average tumor volume and (*C*) individual tumor volume for mice in the control (n = 8) versus N-803 (n = 10) groups. ****$p < 0.0001$ by two-way ANOVA. Flow cytometry was performed on NK cells present within the spleen (*D*) or tumor tissues (*E*) and quantified as a total number of cells within a spleen or per milligram of tumor tissue. Graphs reveal values for each individual mouse displayed in violin plots. Number of total NK cells (defined as $CD45^{POS}$

CD49b^{POS}), NKG2D^{POS}NK cells, and NK cells positive for granzyme B and IFN-γ in (*D*) the spleen or (*E*) the tumor. (*F*) Quantification of mouse IFN-γ levels in plasma collected from mice 48 hours after the final dose of N-803. *$p < 0.05$, ***$p < 0.001$ by unpaired t test in *D* to *F*. In vivo experiment was conducted in two independent times. (*G*) Representative images of tumors stained for expression of MHC-class I. (*H*) Quantification of MFI of human MHC-class I expression in tumors collected at the end of study for mice in control (n = 3) and N-803 treated (n = 8). ***p < 0.001 by unpaired *t* test. ANOVA, analysis of variance; IFN-γ, interferon-γ; MFI, mean fluorescence intensity; NK, natural killer; POS, positive.

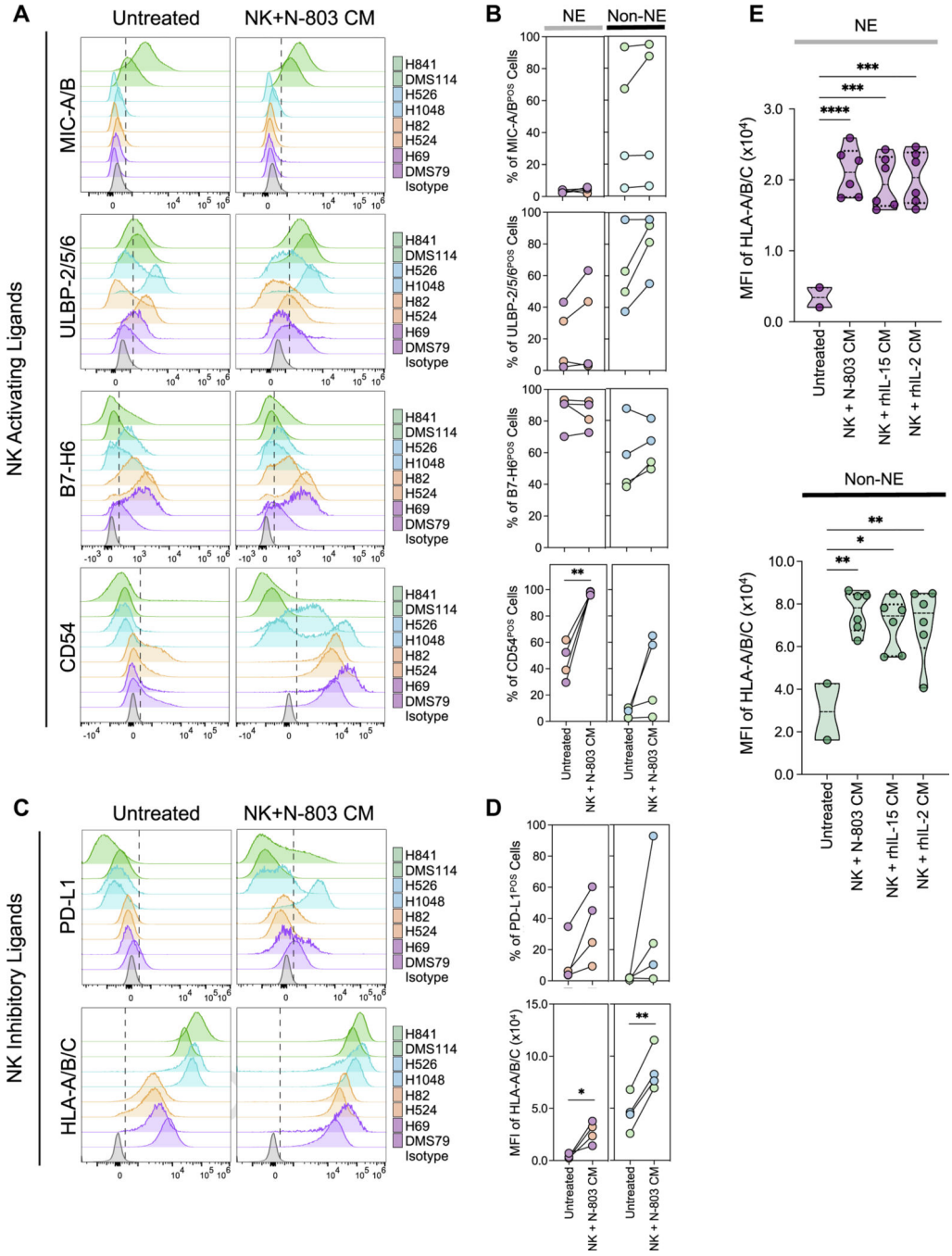

Figure 4.

Expression of NK activating and NK inhibitory ligands on SCLC tumor cells. (*A*) Flow cytometry overlay graphs depicting relative surface expression of NK activating ligands at baseline and postexposure for 48 hours to culture supernatants collected from NK cells activated in the presence of 50 ng/mL N-803 (NK þ N-803 CM). (*B*) Plots displaying the quantification of the percentage of live cells expressing each ligand. NE cells are plotted in the left panel and non-NE on the right. For each cell line, the values at baseline and postexposure to CM are connected by lines representing paired samples. $^{**}p < 0.01$ by

paired t test comparing untreated and CM conditions for all cell lines within each phenotype (NE or non-NE). (*C*) Flow cytometry overlay graphs exhibiting expression of NK inhibitory ligands at baseline and post-CM exposure. (*D*) Quantification of percentage of live cells (PD-L1) or MFI (HLA-A/B/C) before and after exposure to CM. *$p < 0.05$, **$p < 0.01$ by paired t test as described in panel B. (*E*) Quantification of MFI of HLA-A/B/C at baseline and postexposure for 48 hours to culture supernatants collected from NK cells activated in the presence of 50 ng/mL N-803, 15 ng/mL rhIL-15, or 15 ng/mL rhIL-2. (n = 3 NK donors per CM condition, NE plot: DMS79 and H69 cells exposed to CM, non-NE plot: DMS114 and H841 cells exposed to CM). *$p < 0.05$, **$p < 0.01$, ***$p < 0.001$, ****$p < 0.0001$ by one-way ANOVA. ANOVA, analysis of variance; CM, conditioned medium from NK cells treated with N-803; MFI, mean fluorescence intensity; NE, neuroendocrine; NK, natural killer; PD-L1, programmed death-ligand 1; rhIL, recombinant human interleukin.

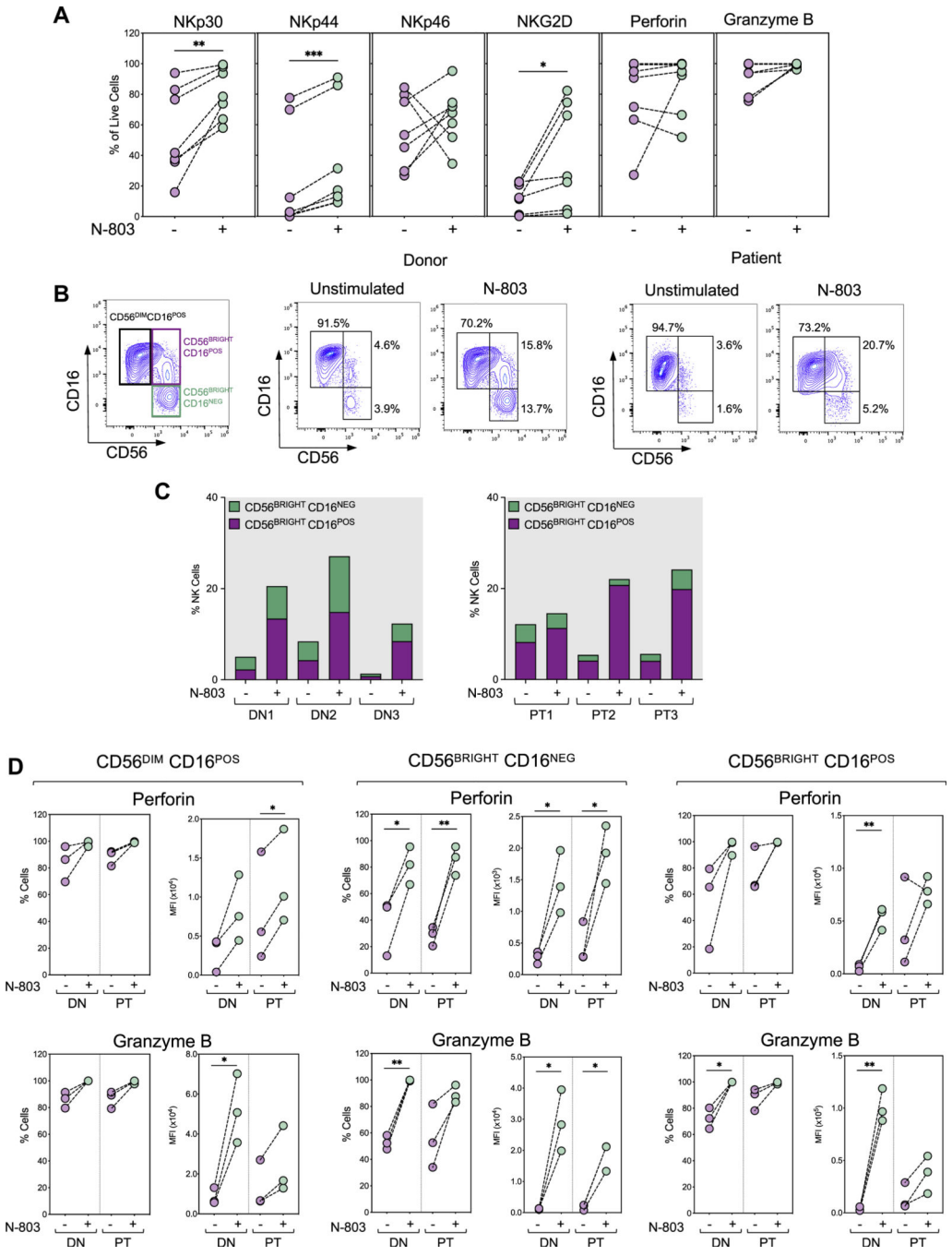

Figure 5.

Effect of N-803 on NK cells from healthy donors and patients with SCLC. (*A*) Quantification of % of live cells expressing each indicated marker, assessed by flow cytometry in NK cells isolated from multiple matched healthy donors with or without N-803 exposure (50 ng/mL for 48 h). Each dot represents a different healthy donor. *$p < 0.05$, **$p < 0.01$, ***$p < 0.001$ by paired *t* test for the comparison of matched NK cells versus NK cells treated with N-803. (*B–D*) PBMC from healthy donors (DN, n = 3) and patients with SCLC (PT, n = 3) were treated with or without N-803 (50 ng/mL for 48 h) before

evaluation by flow cytometry. (*B*) Representative flow cytometry plots depicting gating strategy for NK subsets (left panel) and illustrating a shift in the population of $CD56^{POS}$ NK cells after treatment with N-803 in representative healthy donor (middle panels) and patient samples (right panels). (*C*) Quantification of % NK cells consisting of $CD56^{BRIGHT}$ $CD16^{NEG}$ (green) and $CD56^{BRIGHT}$ $CD16^{POS}$ (purple) subpopulations in indicated samples. (*D*) Quantification of % of cells and MFI for intracellular perforin and granzyme B within identified NK subsets. $*p < 0.05$, $**p < 0.01$ by paired t test for the comparison of matched NK cells versus NK cells treated with N-803. MFI, mean fluorescence intensity; NEG, negative; NK, natural killer; PBMC, peripheral blood mononuclear cell; POS, positive.

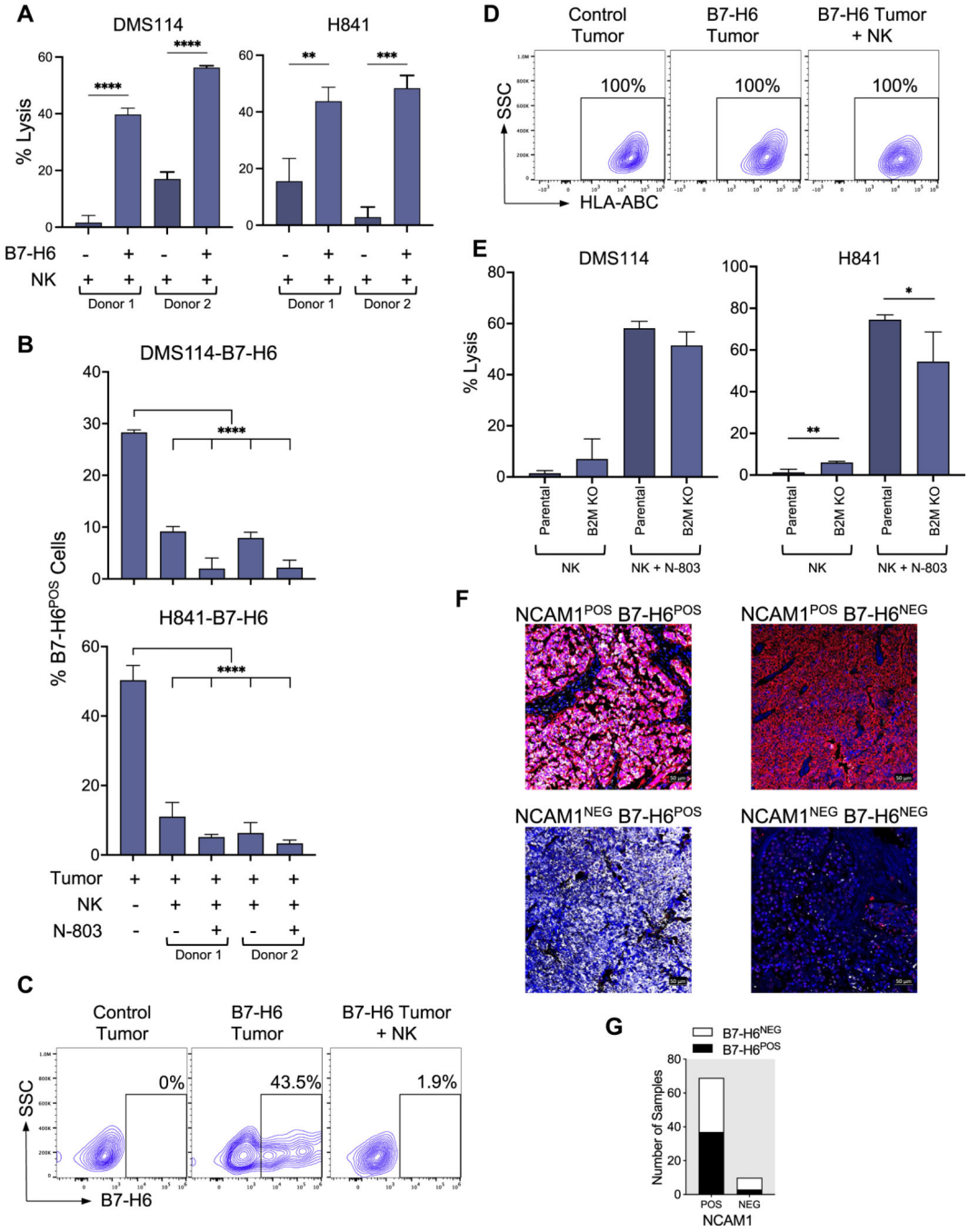

Figure 6.

Lysis of non-NE SCLC cells mediated by the NKp30-B7-H6 axis activation. (A) Lysis assays evaluating susceptibility of target cells transfected to overexpress B7-H6 protein at 6 hours using healthy donor NK cells at an E:T ratio of 20:1. $^{**}p < 0.01$, $^{***}p < 0.001$, $^{****}p < 0.0001$ for the comparison by an unpaired *t* test for each cell line; n = 2 healthy donors. (*B*) Quantification of the % of surviving cells expressing B7-H6 at the conclusion of a 6-hour killing assay using DMS114 or H841 cells transfected to overexpress B7-H6 as targets, and NK cells untreated or treated with N-803 as effectors from two healthy donors

at an E:Tratio of 20:1. ****$p < 0.0001$ by one-way ANOVA compared with the tumor only control. Representative flow cytometry plots revealing the surface expression of (*C*) B7-H6 and (*D*) MHC-class I on H841 cells transfected with a control pCMV6 vector or a plasmid encoding human B7-H6 protein alone or in the presence of NK effector cells. (*E*) Lysis assays evaluating susceptibility of DMS114 and H841 cells modified with CRISPR/Cas9 to knock out B2M and ultimately MHC-class I surface expression, at 6 hours using healthy donor NK cells with or without pretreatment with N-803 (50 ng/mL for 48 h) at an E:T ratio of 20:1. *$p < 0.05$ by unpaired t test comparing parental versus knockout cells for each cell line and each NK condition. Data illustrated are representative of n = 2 healthy NK donors. (*F*) Immunofluorescent staining of NCAM1 and B7-H6 proteins in SCLC tissues of a tumor microarray (NCAM1 = red, B7-H6 = white, DAPI = blue). (*G*) Quantification of SCLC tumors scored based on positivity for NCAM1 and B7-H6 expression. ANOVA, analysis of variance; DAPI, ′,6-diamidino-2-phenylindole; E:T, effector-to-target; NE, neuroendocrine; NK, natural killer.